# Grasper-Needle Coordination in Robotic Laparoscopic Surgery: Potential Fields Approach

Carlos Fontúrbel, Juan Carlos Fraile-Marinero and Javier Pérez-Turiel



November 3, 2023

# GRASPER-NEEDLE COORDINATION IN ROBOTIC LAPAROSCOPIC SURGERY: POTENTIAL FIELDS APPROACH

Carlos Fontúrbel[1], Juan Carlos Fraile[1] and Javier Pérez Turiel[1]

[1] Escuela de Ingenierías Industriales, Medical Robotics Group, Instituto de las Tecnologías Avanzadas de la Producción (ITAP), Universidad de Valladolid, Valladolid, Spain
carlos.fonturbel@uva.es

**Abstract.** This paper proposes a Potential Fields-based approach for coordinating a laparoscopic needle holder and grasper to achieve autonomous suturing in robotic laparoscopic surgery. This method allows seamless transition to teleoperated control based on Virtual Fixtures. The study presents three stages of suture, and experiments conducted in a controlled surgical scenario test the feasibility of the proposed approach. The results indicate successful coordination between the needle holder and grasper, achieving a smooth and logical motion with minimal undesirable effects. The study also discusses challenges such as slow convergence towards attractive points and the need for accurate position determination, suggesting potential solutions and future research directions. Experiments demonstrate successful coordination between the tools, enabling smooth motion with minimal undesirable effects. The approach shows responsiveness and adaptability, promising enhanced autonomous robotic laparoscopy for various surgical tasks.

**Keywords:** Robotic Laparoscopic Surgery, Autonomous Suturing, Potential Fields, Multi-Robot Coordination, Minimally Invasive Surgery.

## 1 Introduction

Laparoscopic surgery is a widely used technique in the current medical context. In these types of interventions, small incisions are made in the patient's abdominal area. Through these openings, any necessary surgical instruments are introduced to carry out the procedure. This minimally invasive surgical technique benefits both the surgeon and the patient, leading to a postoperative recovery with fewer complications [1].

Although laparoscopic surgery, considered a minimally invasive surgery (MIS), addresses many potential problems associated with conventional procedures, it still suffers from several limitations, including restricted maneuverability, limited field of view, and difficulties in navigation due to the trocar's entry point restricting movement. This has made it challenging to achieve a high degree of autonomy for robotic systems in this type of interventions.

Beyond the work carried out with the STAR robot [2], a system with two robotic arms carrying a suturing clamp and a laparoscopic camera, few autonomous robotic systems have been developed, especially in collaborative terms. Furthermore, more research has been conducted on robotic arms collaborating to perform suturing knots [3], but these strategies are not based on a high degree of autonomy, rather on pre-defined optimal trajectory calculations.

On the other hand, it is common to rely on teleoperation as the control system for this type of robotic systems, allowing the surgeon to have complete control over the mobility of the robotic system. Virtual Fixtures [4] consist of generating forces that are applied as feedback in the controller used by the surgeon. These systems were originally designed with the aim of guiding a user in robot manipulation, and their use has been extensively tested as in [5], [6].

Autonomy is a topic to be addressed in the future of robotic laparoscopic surgery. This document proposes a collaborative suturing scenario between the laparoscopic needle holder and a laparoscopic grasper, which must act in parallel, coordinating according to the stage of the process. In the laparoscopic surgery context, autonomy should probably be introduced in the context of task execution, as mentioned by [7]. Furthermore, we believe it is essential to establish a strategy that accommodates both robot autonomy and the option for surgeon teleoperation if needed. Keeping this principle in mind, we propose a specific strategy for the execution of a particular task namely, performing a stitch.

This manuscript presents a strategy aiming to attain a certain level of autonomy while facilitating a smooth transition to teleoperated control at any time. We assess the feasibility of using Potential Fields in this context. This method employs artificial potential (forces) for trajectory planning [8] and has been widely tested for multi-robot systems [9]–[11]. This control is also based on Virtual Fixtures, recently utilized in teleoperated systems [12]. The proposed strategy uses both constraint-based and guideline-based potential fields on the basis of Guidance Virtual Fixtures and Forbidden-Region Virtual Fixtures [13]. This approach enables the integration of various real-world elements, making it compatible with scenarios involving surgical human-robot collaboration, an area that is largely unaddressed and still an open field [14]. The tests to be conducted are intended to verify the feasibility of performing an autonomous suture in a simplified and highly structured surgical scenario, in order to demonstrate the viability of using Potential Fields in this context.

## 2 Materials and Methods

### 2.1 Experimental Setup

Figure 1 shows the experimental setup used throughout these experiments. Two robotic arms, UR3 and UR3e, share a common workspace, allowing the testing of the proposed

autonomous control method, both operating at a control frequency of 10 Hz. Each robot is equipped with a rod-holding tool of 30 cm and 35 cm, respectively, which allows to simulate the position of the tips of both laparoscopic instruments. The rod which simulates the laparoscopic needle holder is controlled by the UR3e robot, while the simulated grasper is controlled by the UR3 robot. It was decided not to limit the workspace with a phantom, and therefore, no restrictions associated with trocars were applied during the initial tests.

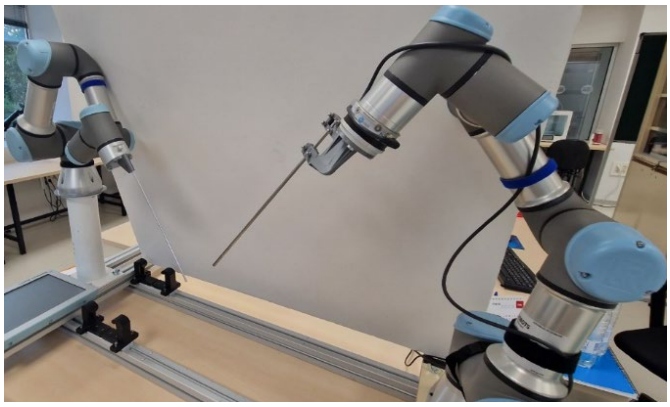

**Fig. 1.** The robotic platform consists of 2 robotic arms, the UR3e and the UR3, each of which is attached to a rod that simulates the position of the tip of the laparoscopic instruments.

The control architecture proposed utilizes the Robot Operating System (ROS) and is depicted in Figure 2. The green blocks represent ROS nodes, with three primary blocks: one for the management and calculus of the autonomous control and one for each robot. The calculations are carried out by the orange intern blocks, while the healthy tissue position is fixed as a parameter, although it may be measured or calculated otherwise.

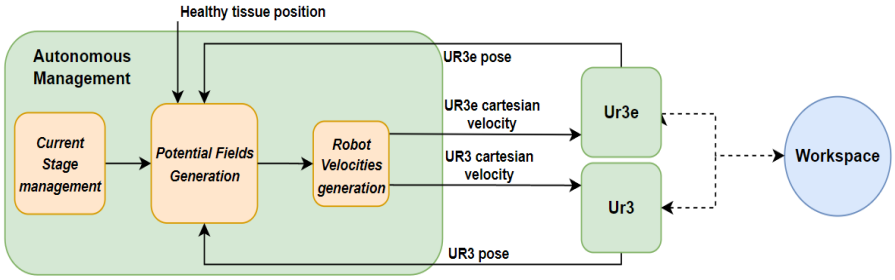


**Fig. 2.** Implementation diagram of the autonomous control carried out in ROS.

## 2.2 General scenario overview

As noted in the early approaches related to the use of Potential Fields in trajectory generation in robotics [15], it is necessary to consider that a workspace with a large number of obstacles will lead to the appearance of local minima, and thus to robot immobility.

We identified and simplified four basic elements of the surgical workspace. These elements include: a cylindrical tool with two protrusions at its end, which simulates the laparoscopic needle holder that will make the incision, another tool with similar characteristics offering simulation of the grasper that will hold the tissue; the healthy tissue; and finally, a target point simulating the suture point to be made.

We have considered that each tool should only be at risk of impact at its TCP, at least in this first iteration of the control method. This simplification is justified due to the highly structured nature of this initial test, where each tool approaches the target point from laparoscopic trocars placed on opposite sides of the abdomen. In this feasibility test, the tools should never cross each other or horizontally approach the trocar through which the opposite tool was introduced. Since the TCP (Tool Center Point) of the robots is theoretically the closest point between them in this test scenario, it is not checked whether the robots collide at a point other than the TCP. The speed of the robot's movement at the TCP is determined solely by its position relative to the other elements in the workspace, but it is not checked whether a manoeuvre is necessary to avoid contact at a point other than the TCP.

### 2.3 Potential Fields guidance

The possible interaction between the different elements has been determined based on 3 different types, depending on the type of interaction they must perform with the laparoscopic tools to be controlled. In situations involving an attractive point, such as suture targets or passage points, a quadratic potential field defined by equation (1) is used.

$$V = 1 - \left(\frac{d}{r}\right)^2; \qquad (1)$$

The goal is to generate a smooth trajectory for the robot, wherein it approaches the target point at a slower pace as it gets closer, but at a higher speed when it is farther from the target point. The value of the potential field $V$ depends on the distance $d$ of the evaluated point from the center of the attractive field. The radius $r$ will be determined on the basis of the distance at which it is desired that the potential is 0, marking the limit of the working area.

Regarding tools, their trajectories must interact with each other to avoid collisions, but not throughout the entire workspace. An excessively wide interaction range can cause the real trajectory to deviate too much from the ideal path and increase the time it takes to reach the target. Similarly, wide potential fields would lead the local minimums away from the target. It is also not advisable to use excessively high gain near the real tool, as it could cause oscillations and undesired movements. To address this, a sigmoid function with low gain is utilized. Around the radius, the slope of this function is maximized, ensuring collision avoidance while receiving information about obstacles from a greater distance. This potential field $V$ is performed using equation (2), where $k$ is the gain, $r$ is the distance where the gradient of this function is maximized,

performing maximum restriction, and $d$ is the actual distance from the analysed point to the center of the potential field.

$$V = \frac{1}{1 + e^{(-k * (r - d))}}; \qquad (2)$$

With this function and applying low gain, each tool provides background information to its counterpart about the workspace, while healthy tissue acts as a virtual barrier with a steeper slope, restricting the workspace for safety without affecting the robots' mobility over long distances.

For healthy tissue, a sigmoid function with higher gain, also known as a *steep* sigmoid, has been used to prevent impacts with this area without overly restricting the tools mobility. Table 1 summarizes the proposed Potential Field associated which each element. The parameters of these potential fields can be adjusted according to the needs of each stage.

**Table 1.** Influence Elements and their associated potential fields in the proposed scenario.

| Influence Element | Potential Field | | Equation |
|---|---|---|---|
| Grasper holder | Cylisphere | Repulsive | Soft Sigmoid |
| Suture needle holder | Cylisphere | Repulsive | Soft Sigmoid |
| Healthy tissue | Prismatic | Repulsive | Steep Sigmoid |
| Target point | Point (Sphere) | Attractive | Quadratic |

## 2.4 Suture Stages

To achieve a suture, a three-stage sequence, along with a resting situation, is proposed. Beginning from the resting state, tools are positioned proximal to the suture. This stage also serves as default state in emergency situations.

**Table 2.** Interaction between the elements at the workspace in the suture Stages (R, repulsive; A, attractive).

| Stage | Tool | RoI | Healthy tissue | Target point | Rest point | Needle | Grasper |
|---|---|---|---|---|---|---|---|
| Stage 0: Rest | Needle | Master | R | --- | A | --- | --- |
| | Grasper | Slave | R | A | | R | |
| Stage 1: Approaching and stitch | Needle | Master | R | A | --- | --- | --- |
| | Grasper | Slave | R | --- | A | R | --- |
| Stage 2: Grasper pressure on the healthy tissue | Needle | Master | R | --- | A | --- | --- |
| | Grasper | Slave | R | A | --- | R | --- |
| Stage 3: Needle Retraction | Needle | Slave | R | A | --- | --- | R |
| | Grasper | Master | --- | --- | --- | --- | --- |

**Stage 0: Resting**

In this stage, both tools need to rest near the target point. One of them, specifically the needle-carrying tool, will act as the master and will remain unaffected by the potential field of the grasper, acting as a slave. The master tool will have its independent resting point, which will be determined during experimentation, always maintaining a safe distance from the suture point. On the other hand, the slave tool will not have its own resting point; its final position will be the outcome of the potential fields that influence it, as illustrated in Table 2.

Consequently, both tools are repelled by the healthy tissue, thereby preventing any interference with it. They also interact with each other in a master-slave configuration, with the master tool, carrying the critical instrument, being subject to more controlled movements to avoid high velocities or accelerations due to potential interactions with the grasper.

**Stage 1: Approach and stitch**

During this stage, the needle holder device approaches and simulates a stitch at the designated target point. The laparoscopic grasper must, therefore, step back from the path of the needle and once again act as the slave tool. This transition occurs simply by maintaining the same potential fields as previously expressed.

To prevent the slave tool from becoming trapped in a local minimum and consequently executing circular motions around the master tool, a resting point is strategically placed close to the target point but in proximity to the trocar associated with the slave tool. This potential field follows a quadratic nature, resulting in a low gradient near the target point. As a result, when the master tool approaches, it induces the slave tool to move towards a safer area, as presented at Figure 3 A).

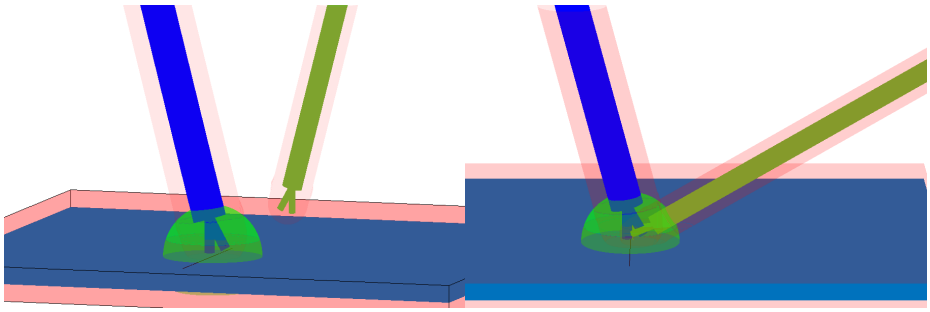

**Fig. 3. A)** Expected equilibrium position for each tool at Stage 1. **B)** Representation of the Stage 2, where both tools must occupy the same workspace.

**Stage 2: Grasper pressure on healthy tissue**

During this stage the master tool position remains stationary, holding the tissue firmly with its closed jaws. Meanwhile, the laparoscopic grasper moves to apply pressure to the tissue at an experimentally determined distance in the direction of the subsequent suture points, where the incision is still open.

In this situation, all potential fields must serve as virtual walls for the robot, for which the Steep Sigmoid function was used. This ensures that the potential field associated with the ground allows pressure to be applied to the healthy tissue up to 3 mm, while strictly prohibiting penetration beyond 5 mm. These defined parameters must govern the behavior of the potential fields. It is important to note that the attractive potential field also helps to prevent the slave tool from descending below the level of this specific point. Figure 3 B) illustrates how the tools interact at this stage.

**Stage 3: Needle Retraction**

In the context of laparoscopic surgery, the needle often retains a portion of the tissue after performing a stitch. Consequently, ensuring a smooth retraction movement by the laparoscopic needle holder while the grasper maintains pressure on the tissue acquires relevance. In this scenario, the needle holder assumes the role of the slave, necessitating careful avoidance of collisions with the grasper or the tissue during the retraction process.

The proposed motion for the needle involves a deliberate retraction from the suture site to a designated resting point along its longitudinal direction. During this movement, the needle is subject to the influence of the potential fields associated with the healthy tissue and the grasper, effectively preventing any contact with these obstacles.

# 3 Results

The stitch was tested according to the proposed sequence using the experimental setup shown in Figure 1. The aim of these tests was to determine whether this approach could potentially allow the execution of an autonomous stitch within this workspace. The speed of each robot was the result of the potential fields affecting it according to the equations shown in point 2.3. A gain of 0.01 was applied to the resulting potential field gradient, limiting the maximum speed to 8 mm/s. All the potential fields related with the attractive points have been settled with the radium $r$ at 1 in eq. (1). Therefore, the gradient caused by the attractive points have a low value near the attractive point.

## 3.1 Stage 0

Stage 0 was tested according to the predetermined experimental design, using a $k$-factor of 200 for the sigmoid function associated with the healthy tissue, while its $r$-factor,

associated with the horizontal deviation of the sigmoid, has been set to 0.2m. This implies that the healthy tissue will influence the position of both tools until the gradient of the potential field is negligible. The value of the distance $d$ where this potential field is $V > 0.999$ is 0.235 m, and the value of the distance $d$ where $V > 0.9999$ is 0.247 m. Both tools remained stationary between 3.8cm and 4.5cm above the tissue, meaning that the potential field is near null in this range. The needle holder, which has an independent attractive rest point, was also affected by this potential field. This effect indicates that the limits of influence of the potential field were working as intended.

The grasper, operating as the slave component, responded to the influence of the needle holder as seen in Figure 4, adjusting its position as the needle approached its rest point. The system required 27s to reach a state of equilibrium. The $k$ factor of the potential field associated with the needle was also set to 200, with an $r$ factor placed at 30 mm, representing the location where the field attained its maximum growth. Consequently, this setup yielded a range of action spanning 44.2mm, ensuring that the grasper maintained a safe distance from the needle.

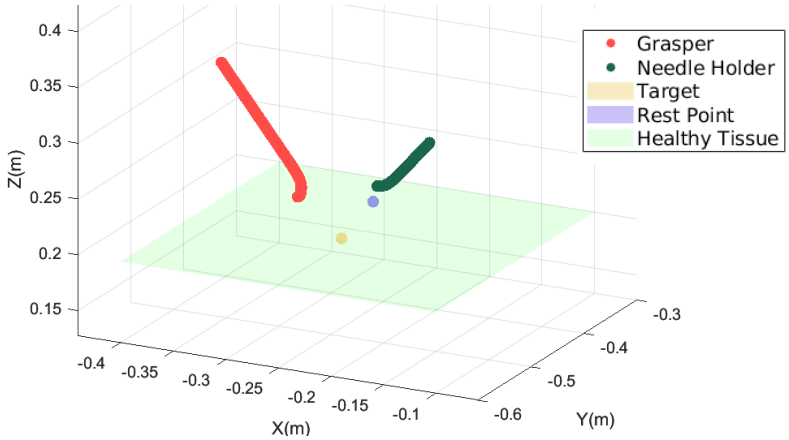


**Fig. 4.** Evolution of the position of the needle and the grasper during Stage 0.

The experiment employed a target point for the grasper situated at [-0.2600, -0.4600, 0.2000], while the needle rest point was [-0.2400, -0.4400, 0.2300]. The final positions of the needle and the grasper were [-0.2367, -0.4391, 0.2442] and [-0.2912, -0.4810, 0.2389], respectively.

### 3.2 Stage 1

Stage 1 shows the impact of the potential field generated by the needle on the grasper, as seen in Figure 5. The $k$-factor associated with the needle potential field was kept at 200, thus affecting the same spatial region as observed in Stage 1. Furthermore, alterations were made to the potential field of the healthy tissue, whereby the k-factor was increased substantially to 1,000. Additionally, the healthy tissue potential field was

displaced by -1.5 cm along the Z axis. The resulting sigmoid generates a virtual wall that won't be surpassed by any of the tools but allows to interact with the tissue. The distance *d* where $V > 0.999$ is 0.192 m, and the value of the distance *d* where $V > 0.9999$ is 0.194 m. Thus, if we consider the real tissue at a Z position of 0.2 m, the potential field permits an interaction range of approximately 5 mm before the repulsion starts.

As a result of these adjustments, the potential field of the healthy tissue no longer affects the grasper. This outcome was expected, as the needle's potential field exerts a repulsive force on the grasper, preventing it from reaching its rest position. To maintain control over the grasper's movement, a rest point was set at [-0.2800, -0.4800, 0.2300].

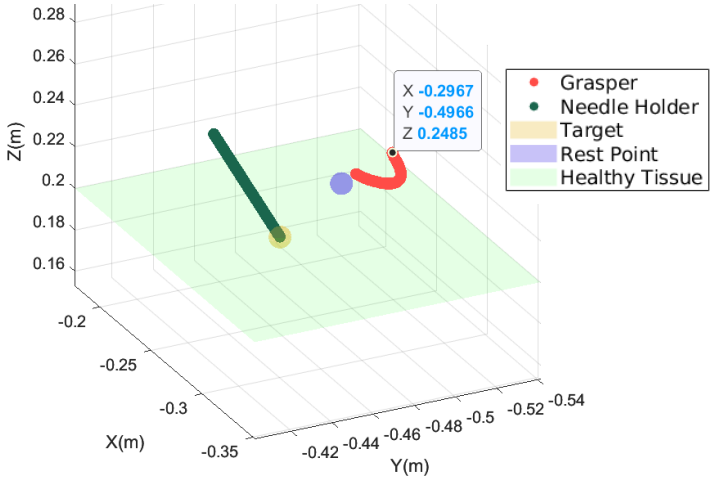


**Fig. 5.** The grasper avoids approaching the needle during this stage.

Throughout Stage 1, the needle pursued its trajectory towards the target point, previously determined as the desired location for the future stitch, a continuation from Stage 0. However, the needle's influence extended to the grasper, impeding it from reaching its predefined rest position. As a consequence, the grasper attained its final position at [-0.297, -0.497, 0.2849]. This indicates that the interaction between the needle's potential field and the grasper's movement has been effectively observed and controlled during the experimental procedures.

### 3.3 Stage 2

This Stage requires cooperation between both tools as seen in Figure 6. The range of this field was reduced by modifying the *r* factor to 10 mm and the k-factor to 2.000. By employing these parameters, a high-growth Potential Field with approximately 15 mm range was generated, originating from the needle holder's symmetry axes. Concurrently, the Potential Field associated with the healthy tissue was maintained from the earlier Stage to safeguard against potential undesired movements.

The rest point for the needle was established at the previous target point, while a new target point was set at the next stitch position, specifically located at coordinates [-0.2600, -0.4600, 0.2000]. The Grasper applies pressure to the tissue, facilitating the progression to Stage 3, where the needle is retracted from the tissue.

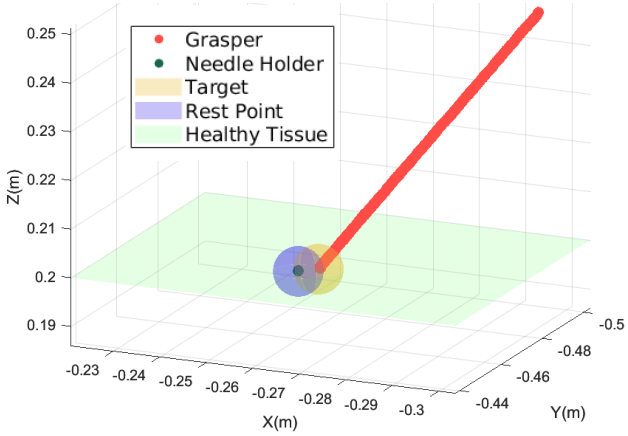


**Fig. 6.** Both tools cooperate in Stage 2, where the grasper must exert pressure on the tissue to allow needle retraction in Stage 3.

### 3.4 Stage 3

In the concluding Stage, the potential fields directly influence the needle as it undergoes retraction, since the constants of the fields were returned to the Stage 0 (default) values. The grasper keeps immobile during this period. This enables a seamless workflow, where both the grasper and the healthy tissue guide the movement of the needle. Consequently, the needle can reach its intended final position while the grasper securely holds the tissue in place. Figure 7 illustrates the movement at this Stage.

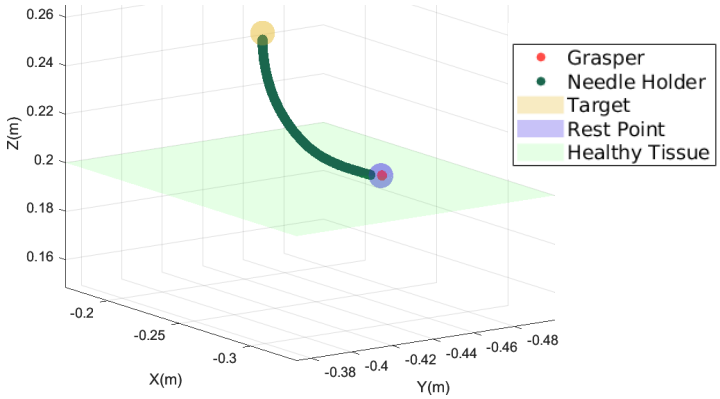


**Fig. 7.** Guided by the Potential Fields associated with the tissue and the grasper, the needle returns to a rest position safely as it detaches from the sutured tissue.

## 4 Discussion and Conclusions

The results obtained from this approach have shown great promise, as evidenced by the performance demonstrated in Section 3 of this manuscript. All stages of the experiment performed as expected, with particularly favorable outcomes observed during Stage 3, where modifications were made to all Potential Fields, whose action was initiated simultaneously. Notably, this adjustment did not lead to any undesirable motion; instead, it resulted in a smooth motion that effectively navigated away from repulsive elements. While these tests yielded several highlights, a few challenges also emerged.

One notable issue was the slow convergence towards the attractive point at each stage, attributed to the quadratic attractive function, which exhibits exponential growth when approaching the attractive point. Addressing this behaviour will be a key aspect in future iterations. Another potential concern lies in the possibility of unpredictable behaviors arising from the elements, leading to unexpected responses from the robot. Although the settings for the potential fields have proven effective within the preestablished workspace, unanticipated movements have not been thoroughly tested. Additionally, accurately determining the real position of the elements, especially the healthy tissue, remains a complex task. Potential solutions, such as the incorporation of a magnetic RGB-D camera, which could be introduced inside the patient and externally controlled, are being explored to overcome this major implementation challenge.

On a positive note, the approach has demonstrated impressive responsiveness and adaptability. Furthermore, its compatibility with teleoperated control based on Virtual Fixtures, an emerging field in robotic laparoscopy, adds to its appeal and demonstrates its alignment with state-of-the-art developments. Although further extensive testing is required, the method holds significant promise for the development of autonomous robotic laparoscopy.

## Acknowledgments

This research was funded by the Spanish Ministry of Science and Innovation through research project PID2019-111023RB-C33 and the Regional Ministry of Education for the pre-doctoral recruitment of research staff co-financed by the European Social Fund (ESF).

## References

[1] B. Rau and M. Hünerbein, “Diagnostic laparoscopy: Indications and benefits,” *Langenbecks Arch Surg*, vol. 390, no. 3, pp. 187–196, Jun. 2005, doi: 10.1007/s00423-004-0483-x.

[2] H. Saeidi *et al.*, “Autonomous Robotic Laparoscopic Surgery for Intestinal Anastomosis,” 2022, doi: 10.1126/scirobotics.abj2908.

[3] B. Lu, H. K. Chu, and L. Cheng, “Dynamic trajectory planning for robotic knot tying,” *2016 IEEE International Conference on Real-Time Computing and Robotics, RCAR 2016*, pp. 180–185, Dec. 2016, doi: 10.1109/RCAR.2016.7784022.

[4] L. B. Rosenberg, “Virtual fixtures: perceptual tools for telerobotic manipulation,” *1993 IEEE Annual Virtual Reality International Symposium*, pp. 76–82, 1993, doi: 10.1109/VRAIS.1993.380795.

[5] J. Ren, R. V. Patel, K. A. McIsaac, G. Guiraudon, and T. M. Peters, “Dynamic 3-D virtual fixtures for minimally invasive beating heart procedures,” *IEEE Trans Med Imaging*, vol. 27, no. 8, pp. 1061–1070, Aug. 2008, doi: 10.1109/TMI.2008.917246.

[6] T. Xia *et al.*, “An integrated system for planning, navigation and robotic assistance for skull base surgery,” *The International Journal of Medical Robotics and Computer Assisted Surgery*, vol. 4, no. 4, pp. 321–330, Dec. 2008, doi: 10.1002/RCS.213.

[7] G. P. Moustris, S. C. Hiridis, K. M. Deliparaschos, and K. M. Konstantinidis, “Evolution of autonomous and semi-autonomous robotic surgical systems: a review of the literature,” *The International Journal of Medical Robotics and Computer Assisted Surgery*, vol. 7, no. 4, pp. 375–392, Dec. 2011, doi: 10.1002/RCS.408.

[8] J.-C. Latombe, *Robot Motion Planning*. Kluwer Academic Publishers, 1991. doi: 10.1007/978-1-4615-4022-9.

[9] J. C. Fraile, C. J. J. Paredis, C. H. Wang, and P. K. Khosla, “Agent-based planning and control of a multi-manipulator assembly system,” *Proc IEEE Int Conf Robot Autom*, vol. 2, pp. 1219–1225, 1999, doi: 10.1109/ROBOT.1999.772528.

[10] J. L. Baxter, E. K. Burke, J. M. Garibaldi, and M. Norman, “Multi-robot search and rescue: A potential field based approach,” *Studies in Computational Intelligence*, vol. 76, pp. 9–16, 2007, doi: 10.1007/978-3-540-73424-6_2/COVER.

[11] P. Song and V. Kumar, “A potential field based approach to multi-robot manipulation,” *Proc IEEE Int Conf Robot Autom*, vol. 2, pp. 1217–1222, 2002, doi: 10.1109/ROBOT.2002.1014709.

[12] T. Xia, A. Kapoor, P. Kazanzides, and R. Taylor, “A constrained optimization approach to virtual fixtures for multi-robot collaborative teleoperation,” pp. 639–644, Dec. 2011, doi: 10.1109/IROS.2011.6095056.

[13] J. J. Abbott and A. M. Okamura, “Virtual fixture architectures for telemanipulation,” *Proc IEEE Int Conf Robot Autom*, vol. 2, pp. 2798–2805, 2003, doi: 10.1109/ROBOT.2003.1242016.

[14] C. Fontúrbel, A. Cisnal, J. C. Fraile-Marinero, and J. Pérez-Turiel, “Force-based control strategy for a collaborative robotic camera holder in laparoscopic surgery using pivoting motion,” *Front Robot AI*, vol. 10, 2023, doi: 10.3389/frobt.2023.1145265.

[15] O. Khatib, “Real-time obstacle avoidance for manipulators and mobile robots,” *Proc IEEE Int Conf Robot Autom*, pp. 500–505, 1985, doi: 10.1109/ROBOT.1985.1087247.